

Subwavelength waveguide for visible light

Authors: J. Rybczynski, Krzysztof Kempa, A. Herczynski, Y. Wang, Michael Naughton, Zhifeng Ren, Z.P. Huang, D. Cai, M. Giersig

Persistent link: <http://hdl.handle.net/2345/bc-ir:107157>

This work is posted on [eScholarship@BC](#),
Boston College University Libraries.

Published in *Applied Physics Letters*, vol. 90, no. 2, 2007

This article may be downloaded for personal use only. Any other use requires prior permission of the author and AIP Publishing.



Subwavelength waveguide for visible light

J. Rybczynski, K. Kempa, A. Herczynski, Y. Wang, M. J. Naughton, Z. F. Ren, Z. P. Huang, D. Cai, and M. Giersig

Citation: [Applied Physics Letters](#) **90**, 021104 (2007); doi: 10.1063/1.2430400

View online: <http://dx.doi.org/10.1063/1.2430400>

View Table of Contents: <http://scitation.aip.org/content/aip/journal/apl/90/2?ver=pdfcov>

Published by the [AIP Publishing](#)

Articles you may be interested in

[Total absorption of light in sub-wavelength metallic waveguides](#)

Appl. Phys. Lett. **103**, 231113 (2013); 10.1063/1.4844655

[A balanced composite backward and forward compact waveguide based on resonant metamaterials](#)

J. Appl. Phys. **109**, 07A319 (2011); 10.1063/1.3554268

[Study of geometrical effects on the characteristics of metallic double-walled carbon nanotube waveguides through quantum hydrodynamics](#)

Phys. Plasmas **16**, 063501 (2009); 10.1063/1.3142468

[Addendum: "The 'needle beam': Beyond-diffraction-limit concentration of field and transmitted power in dielectric waveguide" \[Appl. Phys. Lett.89, 141103 \(2006\)\]](#)

Appl. Phys. Lett. **91**, 089903 (2007); 10.1063/1.2772661

[X-ray waveguide nanostructures: Design, fabrication, and characterization](#)

J. Appl. Phys. **101**, 054306 (2007); 10.1063/1.2435943

The image shows the cover of an Applied Physics Reviews journal issue. It features a blue and orange color scheme with a molecular structure background. The text 'NEW Special Topic Sections' is prominently displayed in white. Below it, 'NOW ONLINE' is written in orange, followed by the title 'Lithium Niobate Properties and Applications: Reviews of Emerging Trends' in white. The AIP Applied Physics Reviews logo is in the bottom right corner.

NEW Special Topic Sections

NOW ONLINE
Lithium Niobate Properties and Applications:
Reviews of Emerging Trends

AIP Applied Physics
Reviews

Subwavelength waveguide for visible light

J. Rybczynski, K. Kempa,^{a)} A. Herczynski, Y. Wang, M. J. Naughton, and Z. F. Ren
Department of Physics, Boston College, Chestnut Hill, Massachusetts 02467

Z. P. Huang and D. Cai
NanoLab Inc., Newton, Massachusetts 02458

M. Giersig
Center of Advanced European Studies and Research (CAESAR), 53175 Bonn, Germany

(Received 5 October 2006; accepted 3 December 2006; published online 8 January 2007)

The authors demonstrate transmission of visible light through metallic coaxial nanostructures many wavelengths in length, with coaxial electrode spacing much less than a wavelength. Since the light frequency is well below the plasma resonance in the metal of the electrodes, the propagating mode reduces to the well-known transverse electromagnetic mode of a coaxial waveguide. They have thus achieved a faithful analog of the conventional coaxial cable for visible light. © 2007 American Institute of Physics. [DOI: 10.1063/1.2430400]

Many future nanoscale optical applications could be conceived and enabled if one could propagate light over large distances (\gg wavelength λ) through transmission lines with nanoscopically restricted, subwavelength transverse dimensions ($\ll\lambda$). Fiber optic cables cannot provide such nanoscopic light guiding.¹ Plasmonic nanostructures have been proposed,²⁻⁵ but due to excessive Ohmic losses associated with plasmons in metals, only very short propagation distances (less than 1 μm) have been observed so far.

Conventional radio technology suggests another solution, the *coaxial cable*, which is the most common transmission line for radio and microwaves.⁶ A schematic of a coaxial cable is shown in Fig. 1(a). It consists of a metallic wire of radius r and a coaxial metallic cylinder with inner radius R . A dielectric medium fills the gap in between. The physics of the conventional coaxial cable is well established:^{6,7} (i) the basic transmitted mode is transverse electromagnetic (TEM); (ii) for this mode, the wave impedance of the coax is identical to that of free space filled with the same dielectric medium as in the coax;⁸ (iii) this mode operates at arbitrary frequency (i.e., no cutoff); and (iv) attenuation is dominated by resistive losses in the metal. Previously, light transmission through “one dimensional” waveguides, of which a coax is one example, had been proposed, but heretofore not demonstrated.⁹

In conventional coax theory, it is customary to assume that the electrode metals are nearly perfect, i.e., highly conductive, and the dielectric medium between electrodes is of very low loss. Impedance matching of a coax to free space can be achieved very efficiently by extending the center conductor beyond the coax end, so that it forms an antenna.^{10,11} In this work, we show experimentally that a nanoscopic analog of the conventional coaxial cable, with properly chosen metals for the electrodes and proper electrode dimensions, indeed retains approximately all of the above properties of its conventional macroscale cousin.

In the visible frequency range, conventional coax theory must be modified because of plasma resonances in the metallic electrodes of the nanocoax.^{12,13} Interaction of these resonances with the photons propagating in the nanocoax

leads to new modes, so-called plasmon polaritons.¹⁴ However, it can be easily shown that, in general, plasmon polaritons reduce to the usual TEM modes of the conventional coax for the following conditions: (a) frequency much below the plasma frequency of the metal, $\omega \ll \omega_p$, (b) interelectrode spacing greater than the penetration depth into the metal, $d=R-r \gg \delta_o$, and (c) inner coax electrode diameter greater than a characteristic value, $2r > c/\omega_p$.¹⁵ The corresponding mode dispersion is then $k_x = (\omega/c)\sqrt{\epsilon_2 - i/L}$. The exponential decay of the mode along the propagation direction (due to losses in the metal) is parametrized by the photon propagation length L , a function of r , R , ω , and a loss parameter γ . In the extreme low frequency limit, $\omega \ll \gamma \ll \omega_p$, this reduces to the well-known decay constant of a conventional coax mode, as expected.⁶ In the intermediate frequency range, $\gamma \ll \omega \ll \omega_p$, the mode is still essentially the usual TEM coax mode, but it experiences a much stronger decay.¹⁵

Our nanocoax, shown in Fig. 1(b), is based on a multi-walled carbon nanotube used as the center conductor. These nanotubes are metallic, with plasma frequency $\omega_p \sim 6 \text{ eV}/\hbar$, and losses in the visible range comparable to those in Cu, i.e., $\gamma \approx 0.003\omega_p$.¹⁶ For these nanotubes, $r=50 \text{ nm}$, and thus $2r > c/\omega_p \approx 50 \text{ nm}$. We employ aluminum oxide (Al_2O_3 , $\epsilon_2 = 2.62$ in the visible range)¹⁷ as the transparent dielectric. The thickness of the dielectric is $d=100 \text{ nm}$, which assures that our nanocoax is a subwavelength transmission line,¹⁸ and also that $d=100 \text{ nm} \gg \delta_o \sim 10 \text{ nm}$. For the outer electrode, we chose Cr, whose dielectric constant in the visible range is

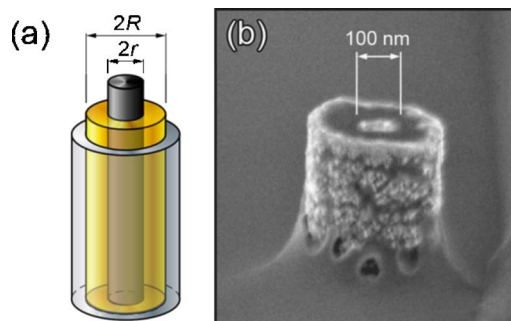


FIG. 1. (Color online) Schematic of a coaxial cable (a) and SEM image of a nanocoax (b).

^{a)}Electronic mail: kempa@bc.edu

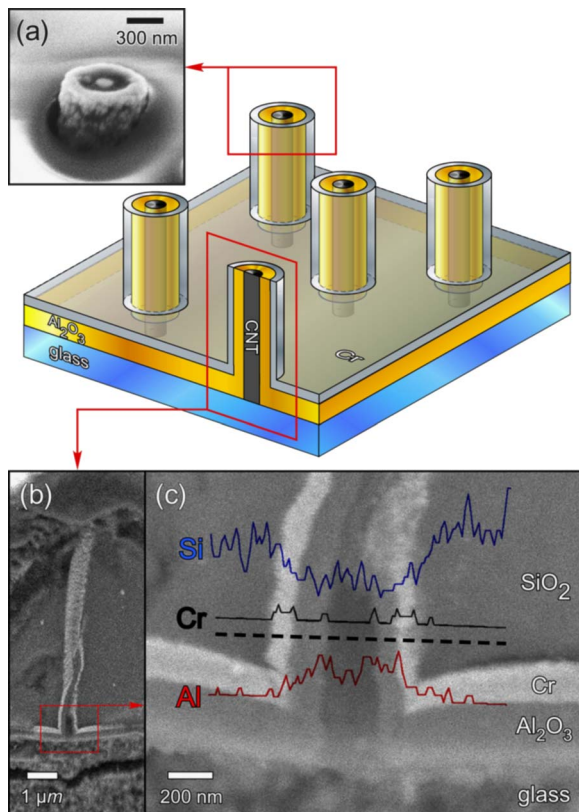


FIG. 2. (Color online) Sketch of nanocoax array, with SEM images of an exposed end of a nanocoax (a), a side view of a nanocoax with open section at substrate revealing layered structure (b), and cross-section view with EDS scans confirming layer composition (c).

$\epsilon_{Cr} = -3 + 18i$, thus well simulating, in the visible, the low frequency dielectric response of a good metal.¹⁴ All these conditions ensure that our nanocoaxes propagate a weakly dispersive mode in the intermediate frequency range ($\gamma \ll \omega \ll \omega_p$), resembling in all respects the conventional TEM coax mode in the visible frequency range, as required. With that, we estimate that the propagation length of light along the nanocoax is $L \approx 50 \mu\text{m}$ in the visible range (i.e., about 10^2 wavelengths). This propagation distance is sufficient for many perceived nanoscale applications.

The nanocoaxes were fabricated as follows. First, an array of vertically aligned carbon nanotubes was grown on glass using plasma-enhanced chemical vapor deposition.^{19,20} A coaxial structure around these metallic nanotubes was built by sputtering Al_2O_3 and then Cr layers. To open the enclosed top ends of the nanocoaxes, the whole array was first filled with spin-on glass and then mechanically polished. Figure 2 shows a sketch of a completed nanocoax array, along with a scanning electron microscope (SEM) image of an entry to a single nanocoax from the polished side, Fig. 2(a). Also shown is a SEM image with a vertical cross section of a single coax, Fig. 2(b), and energy dispersive spectrometry (EDS) scans confirming the composition of each layer, Fig. 2(c). Our completed nanocoaxial array structure consists of a thin film ($\sim 6 \mu\text{m}$) of mostly spin-on glass on a glass substrate, pierced by the nanocoaxes. Due to the presence of the thick, nontransparent Cr coating, light could pass through the sample *only* via the interior of the nanocoaxes, i.e., through the interelectrode spacing ($d = R - r \sim 100 \text{ nm}$) filled with alumina. Note that the inner electrodes of each coax protrude about 250 nm on the substrate side, and thus serve as nanoantennae providing efficient coupling to external radia-

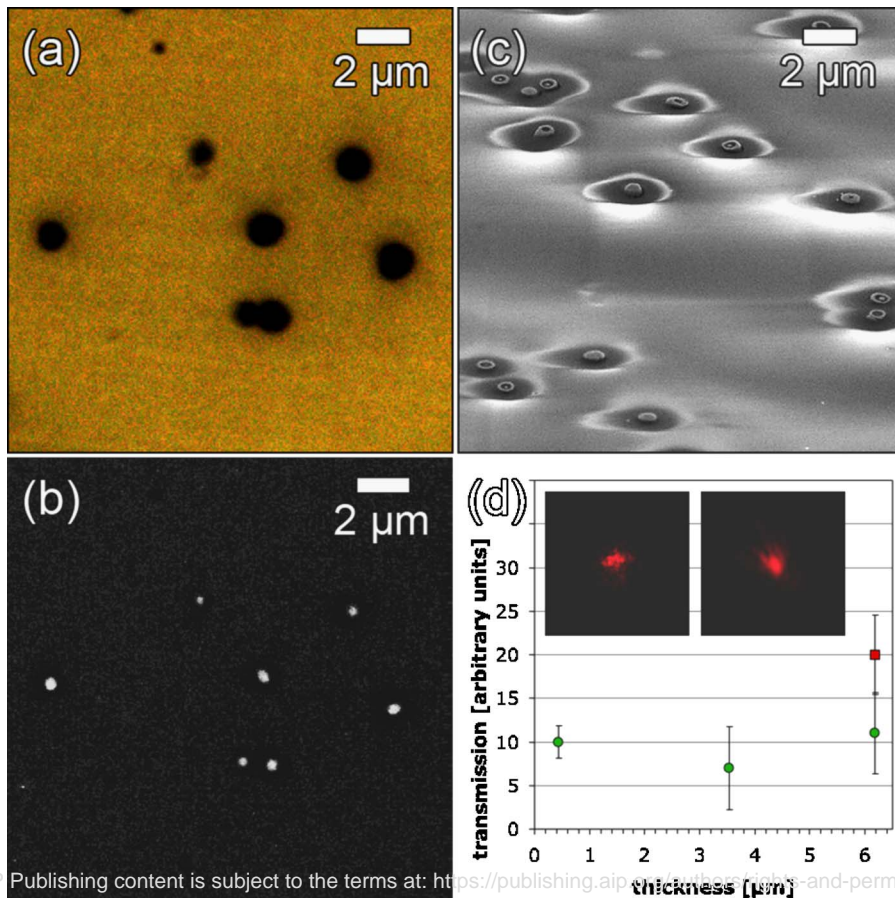


FIG. 3. (Color online) High-resolution optical microscope image of white light reflected from (a), and transmitted through (b) the nanocoax medium. SEM image of medium surface (c) (tilted view). Laser beam transmitted through glass substrate (left), and nanocoax medium on glass (right) (d). Beam diameter $\sim 1 \text{ mm}$, $\lambda = 680 \text{ nm}$. Datum points represent light intensity vs medium thickness (nanocoax length) at 532 nm (green, round) and 680 nm (red, square).

tion. On the polished side, however, there is no antenna section, and thus the overall transmission through a coax is “bottlenecked” by this antennaless end, and is expected to be very small.

Figure 3 shows results of optical reflection from, and transmission through, our nanocoax arrays. In Fig. 3(a), white light is reflected from the top surface of the sample, showing the topography, with dark spots due primarily to absorption of light by the nanocoaxes. When the light is incident from the backside (i.e., that with the antennae), it is transmitted along the coaxes and emerges at the top surface, as seen by the spots in Fig. 3(b) for the same region of this sample. Note that the transmitted light remains white, suggesting there is no cutoff frequency. The SEM image in Fig. 3(c) shows another area of the sample at the same magnification, with a number of nanocoaxes evident.

The above is in agreement with transmission experiments for a much larger area of this sample. In Fig. 3(d), the left inset shows an image of a laser beam ($\lambda=680$ nm) passing directly through the glass substrate,²¹ and projected onto a screen, while the right inset shows the corresponding image for the beam transmitted *through* the nanocoax array. The transmission is subwavelength.¹⁸ The main figure shows that transmission is independent of nanocoax length. Transmission at $\lambda=532$ nm was obtained for various sample thicknesses (i.e., coax lengths). This length independence is fully consistent with our theoretical value for the photon propagation length, $L \approx 50$ μm , which is much greater than each film thickness. There is also no cutoff frequency, since the observed transmission at 680 nm [right inset, and red point in Fig. 3(d)] is even larger than that for shorter wavelength (532 nm, green points). The nanocoax medium is expected to process transmitted light in a discrete manner by breaking the incoming plane wave into wavelets, transmitting it to the other side, and then reassembling the plane wave on the other side of the medium. For straight, identical coaxes, the reassembled wave retains all the propagation characteristics of the incoming wave. This explains the observed lack of beam divergence [beam diameters in the insets of Fig. 3(d) are about the same size]. We have also confirmed all these effects in a macroscopic model of our nanocoax array, by employing conventional radio coaxial cables and microwave frequencies.

Our nanocoax, in addition to being a subwavelength transmission line with obvious applications in nano-optics, also facilitates many novel approaches by enabling subwavelength, nanoscale *manipulation* of visible light. By replacing the interelectrode dielectric with a nonlinear material in each nanocoax, one may achieve light mixing, switching, or phase conjugation.²² The nanocoax structures described here can be fabricated from a wide variety of materials. The inner and outer conductors can be made from any appropriate metal, using soft (e.g., templated electrodeposition, chemical vapor deposition) or hard (electron or focused ion beam lithography) techniques, and the choice of dielectrics is extensive. Moreover, the coupling of radiation (light) to the nanocoax

can be achieved in ways other than the linear antenna described here.

In conclusion, we have designed, fabricated, and tested nanoscale coaxial cables for waveguiding visible light. These nanocoaxes are optically long but radially subwavelength, and they strongly transmit light in the entire visible frequency range, without frequency cutoff. With judicious choice of materials, the propagation is essentially via the conventional TEM mode of a common coaxial cable.

Parts of this work were supported by the US Army Natick Soldier Systems Center under Grant No. DAAD16-03-C-0052. One of the authors (M.G.) acknowledges support by the Deutsche Forschungsgemeinschaft (research unit 557 “Light Confinement and Control with Structured Dielectrics and Metals”), and R. Jarzebinska for help in SEM imaging. Another author (K.K.) acknowledges support by the Massachusetts Technology Transfer Center (2005 Technology Investigation Award).

¹A. W. Snyder and J. D. Love, *Optical Waveguide Theory* (Chapman and Hall, New York, 1983), p. 52.

²W. L. Barnes, A. Dereux, and T. W. Ebbesen, *Nature (London)* **424**, 824 (2003).

³W. J. Fan, S. Zhang, B. Minhas, K. J. Malloy, and S. R. J. Brueck, *Phys. Rev. Lett.* **94**, 033902 (2005).

⁴J. R. Krenn, B. Lamprecht, H. Ditlbacher, G. Schider, M. Salerno, A. Leitner, and F. R. Aussenegg, *Europhys. Lett.* **60**, 663 (2002).

⁵S. A. Maier, P. G. Kik, H. A. Atwater, S. Meltzer, E. Harel, B. E. Koel, and A. A. G. Requicha, *Nat. Mater.* **2**, 229 (2003).

⁶D. M. Pozar, *Microwave Engineering*, 3rd ed. (Wiley, New York, 2005), p. 91.

⁷J. D. Jackson, *Classical Electrodynamics*, 3rd ed. (Wiley, New York, 1998), p. 352.

⁸The wave impedance is not to be confused with the characteristic impedance of a transmission line (see Refs. 6 and 7 for more details).

⁹J. Takahara, S. Yamagishi, H. Taki, A. Morimoto, and T. Kobayashi, *Opt. Lett.* **22**, 475 (1997).

¹⁰K. W. Leung, *IEEE Trans. Antennas Propag.* **48**, 1267 (2000).

¹¹K. Fujimoto, A. Henderson, K. Hirasawa, and J. R. James, *Small Antennas* (Wiley, New York, 1988), p. 209.

¹²M. Ibanescu, Y. Fink, S. Fan, E. L. Thomas, and J. D. Joannopoulos, *Science* **289**, 415 (2000).

¹³F. Forstmann and R. R. Gerhardts, *Solid State Phys.* **22**, 291 (1982).

¹⁴G. Burns, *Solid State Physics* (Academic, New York, 1985), p. 476.

¹⁵K. Kempa (unpublished).

¹⁶Y. Wang, K. Kempa, B. Kimball, J. B. Carlson, G. Benham, W. Z. Li, T. Kempa, J. Rybczynski, A. Herczynski, and Z. F. Ren, *Appl. Phys. Lett.* **85**, 2607 (2004).

¹⁷T. S. Eriksson, A. Hjortsberg, G. A. Niklasson, and C. G. Granqvist, *Appl. Opt.* **20**, 2742 (1981).

¹⁸Note that the longest wavelength of light used in the experiments was $\lambda=680$ nm. It was reduced inside the nanocoax to $\lambda'=\lambda/\sqrt{\epsilon_2}=420$ nm, but this is still *much greater* than the thickness of the Al_2O_3 dielectric, 100 nm.

¹⁹Z. F. Ren, Z. P. Huang, J. W. Xu, J. H. Wang, P. Bush, M. P. Siegal, and P. N. Provencio, *Science* **282**, 1105 (1998).

²⁰Z. P. Huang, D. L. Carnahan, J. Rybczynski, M. Giersig, M. Sennett, D. Z. Wang, J. G. Wen, K. Kempa, and Z. F. Ren, *Appl. Phys. Lett.* **82**, 460 (2003).

²¹A 400 times shorter exposure time was used in the left image, to compensate for the intensity difference between the images due to lack of an antenna on one side of the nanocoax.

²²Y. Chan, H. R. Fetterman, I. L. Newberg, and S. K. Panaretos, *Int. J. Mod. Phys. E* **46**, 1910 (1998).